

# RSC Advances



This is an *Accepted Manuscript*, which has been through the Royal Society of Chemistry peer review process and has been accepted for publication.

*Accepted Manuscripts* are published online shortly after acceptance, before technical editing, formatting and proof reading. Using this free service, authors can make their results available to the community, in citable form, before we publish the edited article. This *Accepted Manuscript* will be replaced by the edited, formatted and paginated article as soon as this is available.

You can find more information about *Accepted Manuscripts* in the [Information for Authors](#).

Please note that technical editing may introduce minor changes to the text and/or graphics, which may alter content. The journal's standard [Terms & Conditions](#) and the [Ethical guidelines](#) still apply. In no event shall the Royal Society of Chemistry be held responsible for any errors or omissions in this *Accepted Manuscript* or any consequences arising from the use of any information it contains.

**Bioactive Ti alloy with hydrophilicity, antibacterial activity and cytocompatibility****Vinod Prabu<sup>1,\*</sup>, P. Karthick<sup>1,\*</sup>, Archana Rajendran<sup>1</sup>, Duraipandy Natarajan<sup>2</sup>,****M. S. Kiran<sup>2</sup> and Deepak K. Pattanayak<sup>1,†</sup>**<sup>1</sup>CSIR-Central Electrochemical Research Institute, Karaikudi, TamilNadu, 630006, India<sup>2</sup>CSIR-Central Leather Research Institute, Chennai, TamilNadu, 600020, India**ABSTRACT:**

Titanium - 6 Aluminium - 4 Vanadium (Ti64) alloy was modified to a hydrophilic, cytocompatible, antibacterial and bioactive surface via a simple cost effective chemical treatment method. A fine porous network structure of sodium hydrogen titanate (SHT) was formed on Ti64 alloy surface by using sodium hydroxide treatment. The incorporated Na<sup>+</sup> ions are replaced by Ag<sup>+</sup> ions by subsequent silver nitrate treatment. Contact angle measurement indicated that silver containing Ti64 alloy surface is hydrophilic at lower silver concentration. The antibacterial study of thus prepared sample against *Staphylococcus aureus* confirmed the bacterial resistance of Ti64 alloy. As evident from AAS result, the sustained release of Ag into the culture medium results in antibacterial activity. Cytocompatibility studies on MG63 cell lines showed above 80% cell viability and also good cell attachment. This confirmed the nontoxic behavior of present optimized silver concentration on Ti64 surface for MG63 cells. *In vitro* bioactivity of silver containing Ti64 sample in simulated body fluid showed bone-like apatite formation and the apatite-forming ability is not affected by Ag concentration or by heat treatment. Taken together, this surface modification study adds further information to our knowledge on development of bioactive Ti64 alloy with hydrophilicity, antibacterial property and biocompatibility that may have considerable potential application as orthopedic and dental implants.

**KEYWORDS:** Ti64 alloy; bioactivity; SBF; antibacterial study; chemical treatment.

---

\*Both the authors have equal contribution to the paper

†Corresponding author E-mail: deepak@cecric.res.in, Ph No - +91-4565-241397

## Introduction

Biomaterials are class of materials that interact with biological systems and help to replace any damaged tissues or organs of the body<sup>1, 2</sup>. Materials such as metals, ceramics, polymers or their combinations are used for fabrication of man-made biomaterials. Among them, metallic biomaterials are very often useful in orthopedic devices such as artificial hip joints, knee joints, spine, bone plates and dental devices<sup>3</sup>. The metals used in this respect are stainless steel, cobalt-chromium alloys, titanium and its alloys. Among them, Ti and its alloys have good biocompatibility, better mechanical properties and high corrosion resistance<sup>4</sup>. Apart from the above properties, Ti and its alloys have excellent fatigue and wear resistance and comparable modulus of elasticity to that of human bone<sup>5</sup>.

Although, Ti and its alloys are biocompatible, new bone formation directly in contact with the implant takes very long time<sup>6</sup>. This necessitates the researcher to develop bioactive Ti and Ti alloys through various surface modifications that can enhance the osteointegration. These surface modifications can be achieved by mechanical methods such as machining<sup>7-11</sup>, polishing<sup>12</sup>, grinding and blasting<sup>13-16</sup> or chemical methods such as chemical treatment, CVD, electrochemical and biochemical etc<sup>7</sup> or by physical modification methods like thermal spraying and physical vapor deposition.

Among various well known chemical modification approaches, acid treatment<sup>17-19</sup>, alkali treatment<sup>20-24</sup>, hydrogen peroxide treatment<sup>25-27</sup>, heat treatment<sup>28</sup> and passivation treatment<sup>29</sup> are well documented in the literature. Although bioactivity could be enhanced by the above methods, colonization of the medical device with bacteria may lead to infection<sup>30</sup>. Despite significant advances in microbiology, this is still one of the

major problems to all medical devices, which may lead to severe pain and secondary surgery depending on the location and type of device<sup>30,31</sup>.

Thus, it could be visualized that Ti and Ti alloys have potential to come out as a biocompatible, bioactive and an antibacterial biomaterial if proper surface chemical treatment is provided prior to the implantation. Although bioactivity could be achieved by various chemical treatment methods, antibacterial property coupled with bioactivity to the implant surface is still a challenge<sup>27</sup>. Several strategies are reported for attributing antibacterial behavior to the material, they include coatings loaded with antibiotics<sup>32-34</sup>, coatings containing non antibiotic organic antimicrobial agents<sup>35</sup>, inorganic antimicrobial agents<sup>36-39</sup>, biofunctionalization with antibacterial bioactive polymers<sup>40</sup>. However, the antimicrobial agent may have adverse effect on human cells due to its low biocompatibility and cytotoxicity<sup>41</sup>. Hence there is a pressing need to have an antimicrobial agent that should show both low cytotoxicity as well as good antibacterial behavior.

Recently literature reports the surface modification approaches to provide bioactivity coupled with antibacterial activity on Ti and Ti alloy<sup>42-45</sup>. This includes antibacterial activity of nanostructured silver titanate against methicillin resistant *Staphylococcus aureus*<sup>42</sup>. However, they have not discussed the bioactivity and cytocompatibility of thus developed silver titanate thin film. Since silver is cytotoxic at higher concentrations, cytocompatibility study of silver substituted samples are inevitable. On the other hand, the titanate - silver nanoparticle - titanate sandwich structure developed on Ti surface with an antibacterial activity and cytocompatibility is reported by Ren et al.<sup>43</sup>. Similar experiment is reported on silver nanoparticle filled nanotube layer on Ti surface<sup>44</sup>. Silver incorporation on Ti and Ti64 alloy surface after hydrogen peroxide treatment for increased surface properties have also been proposed<sup>27</sup>.

<sup>45</sup>. Only limited amount of apatite were observed on such surfaces even after 15 days soaking in simulated body fluid<sup>45</sup>. In the present investigation, *in vitro* bioactivity, antibacterial activity and cell compatibility of silver incorporated Ti64 alloy with respect to the silver concentration was systematically examined.

## 2. Experimental

### 2.1 Preparation of samples

Ti64 alloy rod of diameter 15 mm was cut into circular samples of thickness 1 mm, and abraded with # 400 SiC paper to remove the oxide layer formed on its surface. The polished samples were then washed in sequence with acetone, 2-propanol, and ultra-pure water, respectively for 15 min each in an ultrasonic cleaner. The cleaned samples were dried in an oven at 40 °C for overnight. The dried samples were immersed in 10 mL of 5 M NaOH (Sigma Aldrich, purity 98 %) solution under shaking at 120 rpm at 60 °C for 24 h. After removal from sodium hydroxide solution, the samples were washed with ultra-pure water, to remove the weakly bonded Na<sup>+</sup> ions. These samples were subsequently soaked in AgNO<sub>3</sub> (Sigma Aldrich, purity 99.8 %) solution of different concentrations ranging from 0.01-100 mM under shaking at 120 rpm at 40 °C for 24 h. Silver incorporated samples were then gently washed with ultra-pure water and allowed to dry in an oven. Some of the samples were heat treated at 600 °C for 1 h in air atmosphere and the rate of heating was maintained at 5 °C / min. Table 1 shows the notations of various chemical and thermal treatments used in the present study.

### 2.2 Surface analysis of chemically treated Ti64 alloys

The surfaces of the Ti64 alloy subjected to various chemical treatments described above were observed using scanning electron microscope (SEM; TESCAN, Czech Republic). The chemical composition of surfaces of chemically treated Ti64 alloy were

analyzed by energy dispersive X-ray spectroscopy analysis (EDX) attached to the SEM under an acceleration voltage of 15 kV. This analysis was carried out in three different location of each sample and averaged to know the amount of silver ions incorporated into the Ti64 alloy. In order to identify the surface functionalization, laser Raman spectroscopy (RENISHAW Co., UK) was used for Ti64-N-0.05 to 100Ag sample before and after heat treatment. For this measurement, He-Ne Laser with a wavelength of 630 nm was used.

X-ray diffraction (XRD) analysis was carried out to observe the differences in the crystallographic structure for the Ti64-N and Ti64-N-100Ag samples before and after heat treatment. XRD measurements were made on a Bruker D8 Advance diffractometer in Cu K $\alpha$  radiation and detected using a Bruker Lynx Eye detector. XRD spectra were recorded in the range 10-60° in 2 $\theta$  at a step size of 0.02° and a count time of 5 s. Chemical state and composition of Ag containing Ti64 alloy after heat treatment was investigated by X-ray photoelectron spectroscopy (XPS; Thermo V G Scientific, UK). All XPS data presented here were acquired using Al K $\alpha$  line 1486.6 eV. The photoelectrons were collected at an electron take off angle of 45 °C. Peak positions were then calibrated with respect to the C<sub>1S</sub> peak at 284.5 eV. Silver release in SBF was measured by atomic absorption spectrophotometer (AAS; Varian Co., Australia). Surface morphology of Ti64 alloy subjected to chemical and heat treatment and soaked in SBF was similarly characterized by SEM and XRD.

### *2.3 Contact angle study*

Wetability (extent of hydrophilicity / hydrophobicity) of various chemically treated Ti64 surfaces was evaluated by contact angle measurement, VCA Optima instrument and VCA Optima XC software. Measurements were carried out under static

(equilibrium) mode using distilled water as the test liquid. After proper cleaning the syringe of 100  $\mu$ l capacity, one drop (5  $\mu$ l) of distilled water is put on the sample surface and the water contact angle is recorded by an optical microscope connected with a camera. The measurements were carried out at three different places for each sample and the results were averaged.

#### 2.4 Antibacterial study

Zone of inhibition method was used to evaluate the antimicrobial properties of Ti64, Ti64-N, Ti64-N-0.01 to 100Ag samples. For antimicrobial activity study, the procedure reported earlier was followed<sup>27</sup>. In brief, 200 mL of nutrient medium was prepared with sterile distilled water in a conical flask and then autoclaved at 121 °C for 15 min. Then at the hand bearable heat the sterilized nutrient medium was poured aseptically into the sterile petriplates and allowed it to solidify. After solidification, the plates were kept in an inverted position to avoid the formation of water droplets inside the plates. Lyophilized cells of *Staphylococcus aureus* were collected from Microbial Type Culture Collection and Gene Bank (MTCC), Dept. of Biotechnology, Chandigarh, India. The vials were cut open and the lyophilized cells were aseptically transferred into the nutrient broth (0.5% NaCl, 0.15% yeast extract, 0.15% beef extract, 0.5% peptone) at room temperature and incubated at 37 °C for about 24 h. The overnight culture of *Staphylococcus aureus* were taken and the cells were swabbed on the nutrient agar plates using sterile cotton swab under sterile condition to avoid the over growth of cells and contamination. All the treated Ti64 alloy samples were aseptically placed on the inoculated plates using a sterile forceps and incubated at 37 °C for 24 h.

#### 2.5 Cytotoxicity study:

### 2.5.1 MTT assay

MTT [3-(4, 5-dimethylthiazol-2-yl)-2, 5-diphenyl-tetrazolium bromide] assay was performed to analyze the cytotoxicity of various concentrations of Ag containing samples. MTT assay is based on the metabolic ability of the viable cells to reduce soluble MTT by mitochondrial enzyme into an insoluble color formazan product, which is measured spectrophotometrically<sup>27, 46</sup>. The insoluble formazan is dissolved in dimethyl sulfoxide (DMSO) before subjecting it for spectrophotometric measurement at 560 nm. MG63 cells, 10000 cells / mL were seeded in a 24 well tissue culture multiplates containing Ti64-N-0.02 to 0.1Ag samples. The cells were maintained in DMEM medium in a CO<sub>2</sub> incubator at 37 °C (5 % CO<sub>2</sub> / 95 % atmosphere) for 48 h. Control groups include untreated cells and the sample alone with starting reagents. After 48 h of incubation, the cells were imaged using a Leica Phase contrast microscope. The culture medium was removed and the cells were washed with sterile PBS. The cells were then incubated for 3 h with 250 µl PBS containing MTT (0.5 mg/mL). After 3 h the PBS was removed and the formazan product formed was solubilised in 150 µl of DMSO. The absorbance was measured at 560 nm using BioRad microplate reader<sup>47</sup>. The results given are average of three independent experiments.

### 2.5.2 Cell adhesion study

In order to study the morphology of cells adhered on Ag treated Ti64 surface, cells were allowed to grow on the surface and was observed under SEM after proper fixation. Briefly 20,000 cells (MG63) were seeded on sample surface without overflowing and incubated in a CO<sub>2</sub> incubator at 37 °C, 5% CO<sub>2</sub> and 95 % air for 24 h. After incubation the cells on the sample surface were fixed with 4 % w/w formaldehyde in PBS and incubated for 30 min at room temperature. Further the cells were dehydrated through a series of ethyl alcohol solution (from 50 % to 100 % v/v in distilled water),



followed by a ratio of ethyl alcohol and hexamethyl disilazane solution at 3:1, 1:1 and 1:3 ratios respectively. Sample was air dried and observed in SEM after gold sputtering.

### 2.6 Preparation of simulated body fluid (SBF)

SBF is an acellular solution with ion concentrations (in milli moles:  $\text{Na}^+$  142.0,  $\text{K}^+$  5.0,  $\text{Mg}^{2+}$  1.5,  $\text{Ca}^{2+}$  2.5,  $\text{Cl}^-$  147.8,  $\text{HCO}_3^-$  4.2,  $\text{HPO}_4^{2-}$  1.0,  $\text{SO}_4^{2-}$  0.5) nearly equal to those of human blood plasma at 36.5 °C. The SBF was prepared as per Kokubo protocol by dissolving reagent-grade NaCl, NaHCO<sub>3</sub>, KCl, K<sub>2</sub>HPO<sub>4</sub>·3H<sub>2</sub>O, MgCl<sub>2</sub>·6H<sub>2</sub>O, CaCl<sub>2</sub> and Na<sub>2</sub>SO<sub>4</sub> (Sigma Aldrich, purity 99 %) into ultra-pure water, and buffered at pH 7.4 with tris-hydroxymethylaminomethane(CH<sub>2</sub>OH)<sub>3</sub>CNH<sub>2</sub>) and 1 M HCl (Sigma Aldrich, purity 99%)<sup>48</sup>. The SBF was kept in a refrigerator for 3 to 4 days prior to use.

#### 2.6.1 *In vitro* bioactivity in SBF

In order to analyze the bioactivity, each specimen subjected to chemical and heat treatment was immersed in 30 mL of SBF contained polypropylene centrifuged tube covered with a tight lid and kept in a water bath maintained at a temperature of 36.5 °C for 7 days. Then the samples were removed from the solution, gently washed with ultrapure water and dried for further characterization. The morphology of bone-like apatite formation on the surface of Ti64 alloy surface during the incubation was observed using SEM. All samples were coated with gold prior to SEM observation. The bone-like apatite growth and elemental composition of the growth was also evaluated by using XRD and an EDX detector attached to the SEM, respectively.

#### 2.6.2 Release of Ag<sup>+</sup> ions in SBF

The silver ion released from the sample (Ti64-N-0.05Ag) was estimated in order to study the silver release kinetics. Here, sample was first soaked in 30 mL of SBF and a gentle shaking (50 rpm) was given in order to mimic the body condition<sup>49, 50</sup>. Each time 1 mL of SBF solution was drawn from the 30 mL and replaced with 1 mL fresh SBF so that the total volume remain constant. The 1 mL silver containing SBF solution was dissolved in equal amount of HNO<sub>3</sub> and then diluted 10 times and the amount of silver released were measured by AAS<sup>27</sup>.

### 3. Results

#### 3.1 Scanning electron microscopy and energy dispersive X-ray spectroscopy analysis

Fig. 1 show the SEM photographs of the surface of Ti64 alloy subjected to AgNO<sub>3</sub> treatment of different concentrations after NaOH treatment compared to that of surface of untreated Ti64 alloy and that treated with only NaOH solution. The Ti64 alloy showed a smooth surface with uniform patterns on it, which is formed during polishing with #400 SiC paper while NaOH treated surface showed a fine porous network structure in nanometer scale. This fine porous network structure was retained by the subsequent AgNO<sub>3</sub> solution of different concentrations.

Fig. 2 show the EDX results of Ti64 alloy treated with AgNO<sub>3</sub> solution under various concentrations followed by treatment in NaOH solution. It can be seen from Fig. 2 that the NaOH treatment incorporates about 2 at. % of Na<sup>+</sup> ions in to the Ti64 alloy. The amount of silver content increased with increasing AgNO<sub>3</sub> concentration (about 2.2 at. % for Ti64-N-100Ag sample) while the concentration of Na<sup>+</sup> ions becomes almost negligible. This indicates that most of the Na<sup>+</sup> ions are replaced by the Ag<sup>+</sup> ions by the subsequent chemical substitution process. The amount of silver on NaOH treated Ti64 alloy samples soaked in AgNO<sub>3</sub> solution up to 2 mM is depicted by dotted region in Fig.

2. Initially silver ion incorporation increased with increase in concentration of  $\text{AgNO}_3$  solution, and becomes almost saturated at a concentration of 10 mM.

### 3.2 Raman spectroscopy and X-ray diffraction study

Fig. 3 (a & b) shows Raman spectra of the surfaces of Ti64 alloy after NaOH and NaOH-0.05 to 100 Ag before and after heat treatment. The results showed that sodium hydrogen titanate (SHT) was formed on the surface of NaOH treated alloy sample, the spectrum of each specimen shows a set of five broad peaks at 276, 440, 660-670 and 906  $\text{cm}^{-1}$ , which are found to be in good agreement with earlier reports on hydrogen titanate<sup>51-52</sup>. The intrinsic hydrogen titanate ( $\text{H}_2\text{Ti}_3\text{O}_7$ ) bands at 276 and 906  $\text{cm}^{-1}$  are due to the Ti-O-H bonding<sup>53</sup>. Based on the studies of *Ma et al*<sup>54</sup>, the peak at 440  $\text{cm}^{-1}$  is due to the Ti-O bending vibration involving six-coordinated titanium atoms and three-coordinated oxygen atoms. The peak at 660  $\text{cm}^{-1}$ , according to the studies of *Kasuga et al*<sup>54</sup> and *Sun and Li*<sup>55</sup>, is ascribed to the Ti-O-Ti vibration in  $[\text{TiO}_6]$  octahedral layer in the titanate. On subsequent treatment with  $\text{AgNO}_3$  solution, the sodium ions in SHT are replaced by the silver ions from  $\text{AgNO}_3$  solution and form  $\text{Ag}^+$  containing hydrogen titanate (HT), without any peak shift. On increasing the concentration of  $\text{AgNO}_3$  solution, amount of doped silver on Ti64 alloy surface also increases thereby the peak intensity get reduced<sup>36</sup>. On subsequent heat treatment this SHT and HT layer were converted to sodium titanate and anatase phase, respectively as observed in Fig. 3(b). These results are in good agreement with our previous studies<sup>27, 52</sup>.

Fig. 3 (c) shows the XRD spectra of Ti64-N and Ti64-N-100Ag samples before and after heat treatment. Apart from Ti peaks, small peak of ST was observed at  $24.6^\circ$  in 2 theta. On subsequent treatment with 100 mM  $\text{AgNO}_3$  solution and heat treatment, an

anatase phase was observed along with silver peak ( $44^\circ$  in 2 theta). This shows that during heat treatment  $\text{Ag}^+$  ions are transformed to metallic Ag.

### 3.3 X-ray photoelectron spectroscopy study

In order to understand the state of silver, XPS analysis of Ti64-N-0.05Ag-H sample was carried out and is shown in Fig. 4. The survey scan shows the presence of oxygen, titanium, silver, sodium and vanadium along with carbon peak. Narrow scan of  $\text{Ag}_{3d}$  peak is shown as an inset. Peak corresponding to 367.2eV ( $\text{Ag}^+$ ) indicates silver to be present as  $\text{Ag}_2\text{O}$ . Additional broad peak at 368.1 is assigned to be  $\text{Ag}^0$  state. It is well known that silver on titania surface can easily oxidized in to silver oxide ( $\text{Ag}_2\text{O}$ ).<sup>27</sup>

### 3.4 Contact angle measurement

Fig. 5(a) shows the image of a water droplet when dropped on the surface of untreated Ti64 alloy and chemically treated samples. Distilled water contact with untreated Ti64 alloy at an angle of above  $80^\circ$  shows some amount of hydrophobicity which is evident in the Fig. 5(b). Comparing to Ti64 alloy, Ti64-N showed very low contact angle of  $25^\circ$ . The other images represent the samples treated with  $\text{AgNO}_3$  solution at different concentrations (0.1 to 100 mM) followed by NaOH treatment. Results showed that at lower concentration of silver (0.1 mM), the contact angle is  $18^\circ$  which is less than that of NaOH treated samples and the contact angle increases for increased amount of silver (100 mM) contact angle is  $140^\circ$  which decreases the wettability of Ti64 alloy and increased the hydrophobicity of the surface.

For an ideal biomaterial, it should have a higher wettability along with adequate antibacterial property because a material with better wetness will develop the tissue fragments and easily integrated with the biological system<sup>56, 57</sup>. But it is found in contact angle studies that wettability decreases with increased amount of silver on the surface. So,

the amount of silver deposited on the surface of material needs to be optimized such that the material could have better wettability as well as good antibacterial behavior.

### 3.5 Antibacterial study

Fig. 6 (a-c) shows the antibacterial study of Ti64 alloy and chemically treated samples against *Staphylococcus aureus*. Ti64 alloy and NaOH treated sample did not show any antibacterial activity as shown in Fig 6 (a). From Fig. 6 (b & c) silver treated samples starting from 0.02-0.5 mM shows clear bacterial inhibition zone and the extent of zone formation was increased with increase in silver content. But, the admissible amount of silver ions into the human body is limited because excess silver ions might cause cytotoxicity<sup>58-60</sup>. An attempt has been made to optimize the silver content in an implant material and to determine the minimal silver content, which would be sufficient to produce effective antibacterial effect. So, it could be observed that there was no inhibition zone in the case of samples treated in 0.01 mM Ag solution while a clear inhibition zone could be obtained for 0.02 mM and above AgNO<sub>3</sub> treated specimens. The magnitude of the inhibition zone obtained has been depicted in Table 2.

### 3.6 Silver release study

Fig. 6 (d) shows the concentration of silver ion released in SBF with respect to different immersion time. This study on the rate of release of silver ions, thus leading to anti-bacterial behavior was performed on Ti64 alloy treated with NaOH and 0.05 mM AgNO<sub>3</sub> solution. Release rate of silver increases rapidly during the first 3 h after which the rate of release gets slower and becomes almost constant after 24 h<sup>61, 62</sup>.

### 3.7 Cell culture study

Thus prepared silver containing Ti64 samples were tested for its cytotoxicity using MTT assay. The cytocompatibility for various concentration of Ag ranging from

0.02 to 0.1 mM was evaluated and the results are presented in Fig. 7 (a). The results suggested that above 90% cell viability for AgNO<sub>3</sub> concentration of 0.02 mM, 86% cell viability for 0.03 mM and above 80 % for 0.05 mM. However, it drastically decreased to 43 % for 0.1 mM AgNO<sub>3</sub> treated sample. The results indicated that the cell viability and biocompatibility was not affected at concentration ranging from 0.02 to 0.05 mM Ag indicating the concentration range would find application for biomedical interventions under diseased conditions.

Fig. 7 (b) shows MG63 cells adhered to Ti64-N-0.05Ag sample surface. Cells were uniformly adhering to the surface within 48 h of incubation and most of the cells showed random spreading. Cell attachment, spreading and further proliferation is directly related to surface characteristics of the material. The adherence of MG63 cells to the silver containing Ti64 surface indicates biocompatibility of the present surface and also expected to induce further proliferation of the cells.

### *3.8 In vitro bioactivity study in SBF*

Fig. 8 (a) show the SEM images of Ti64 alloy treated with NaOH and different concentration of AgNO<sub>3</sub> and soaked in SBF for 7 days. Spherical globules were formed on all the NaOH and AgNO<sub>3</sub> treated Ti64 alloy and there was no deposition formed on the untreated Ti64 alloy. Fig.8 (b) shows a typical XRD pattern of Ti64 alloy subjected to NaOH and AgNO<sub>3</sub> treatment and soaked in SBF for 7 days. Ti64 alloy modified with NaOH and AgNO<sub>3</sub> shows peak at 26 and 32° which correspond to the formation of bone like apatite. The remaining peaks correspond to Ti in Ti64 alloy<sup>63, 65</sup>. This indicates that the chemical treatment enhances the apatite forming ability of Ti64 alloy in SBF.

## **4. Discussions**

Metals such as Ti and Ti alloys are used in orthopedic and dental devices for past several decades. However, strong bonding between implant and living bone is always a serious issue when implant needs to remain in the body for longer duration. In order to provide this strong bone-bonding ability in Ti and Ti alloys, either bioactive coating such as calcium phosphates<sup>65</sup> or bioactive chemical treatment<sup>17</sup> are developed. Ti and Ti alloys when subjected to NaOH treatment form a sodium titanate porous layer (Fig. 1) and this sodium titanate release  $\text{Na}^+$  ions into the SBF to form Ti-OH groups. This Ti-OH group accelerates the  $\text{Ca}^{2+}$  and  $\text{PO}_4^{3-}$  ions deposition from SBF to form a bone like apatite as evident in the SEM and XRD results (Figs. 8 (a & b)). It has been reported that if a material form bone-like apatite on its surface in SBF it allows to deposit bone in the living body in the same manner and accelerate the bone integration. Both osteoconduction and osteoinduction abilities are well documented in the literature for various Ti and Ti-Zr-Nb-Ta alloys. However,  $\text{Na}^+$  ion release and its accumulation in the body may cause toxicity to the cells and cell death. In order to avoid such a situation, either water or dil. HCl treatment following NaOH treatment is reported by one of the author<sup>52</sup>. However, NaOH or NaOH- $\text{H}_2\text{O}$ , dil. HCl treatments do not show any antibacterial activity and similar observations are also made in the present study (Fig. 6 (a-c)).

This indicates that thus manufactured orthopedic implant is susceptible to the bacterial infections during the course of surgery. This bacterial infection may lead to puss formation and ultimately the implant failure. In order to overcome this if an antibacterial agent can be impregnated into the porous network structure by chemical reaction; it can address the antibacterial behavior of the implant. Although, various organic compound coated over metallic implant to prevent bacterial infections are already reported, the present manufacturing process involves higher temperature that

may degrade the activity of the organic compound<sup>32-34</sup>. On the other hand, silver is a popularly known antibacterial agent and is being used in various applications<sup>36-37</sup>.

The mechanism of chemical reactions taking place on the surface of Ti64 alloy could be described as follows (considering the major composition of the alloy as Ti). Thus, in the transformation of simple titanate surface to silver substituted hydrogen titanate could be understood in two steps:

- **NaOH treatment** – Ti / TiO<sub>2</sub> surface is attacked by hydroxyl ions to form sodium hydrogen titanate<sup>7</sup>.
- **Ion exchange reaction** – Sodium ions in sodium hydrogen titanate is substituted by silver ions forming silver hydrogen titanate.

According to the EDX results (Fig. 2), the proportions of sodium and silver seem to be interrelated. The maximum amount of sodium observed is 1.91 at % which is found to decrease proportionally with the increase in silver concentration. Although the proportional amount of Na<sup>+</sup> ion is replaced by silver, the amount of sodium present is always lower after ion exchange reaction because the sodium ions are easily washed away while rinsing with water. After a certain amount of incorporated silver, its content becomes saturated due to limited availability of sodium ions for exchange reaction.

The treated Ti64 alloy samples formed a layer of silver titanate on its surface as confirmed by EDX result (Fig. 2). These alloy samples show bactericidal through zone of inhibition tests in which the clear zones could be seen around the samples in the *Staphylococcus aureus* culture medium (Fig. 6 (a-c)). Result showed that Ti64 alloy treated with a concentration above 0.02 mM AgNO<sub>3</sub> has antibacterial effect.

In metallic form, silver is unreactive and cannot kill bacteria. To become bactericidal, silver must lose an electron and become positively charged silver ions



(Ag<sup>+</sup>). Elemental silver ionizes more readily when exposed to an aqueous environment such as in body fluids in the present study. Thus, there is antibacterial effect only when there is a release of silver ions from the implants. The release of silver from the surface modified alloy sample is evident from the AAS studies as seen in Fig. 6 (d). The released silver ions are highly reactive and affect multiple sites within bacterial cells, ultimately causing bacterial cell death. They bind to bacterial cell membranes, causing disruption of the bacterial cell wall and cell leakage. Silver ions incorporated into the cell disrupt cell function by binding to proteins and interfering with energy production, enzyme function and cell replication<sup>59, 62</sup>.

The above mentioned activities lead to the following two major effects on the bacterial cell<sup>59</sup>.

- Due to the detrimental effect of the silver ions the DNA molecules become condensed and lose their abilities to replicate.
- Silver ions interact with the thiol groups in proteins, thus inducing their inactivity<sup>27</sup>.

Contact angle measurement is a study performed to analyze the degree of hydrophobicity or hydrophilicity of the material of desire. This contact angle study is performed to analyze the wettability of the surface modified alloy samples. This would give an idea about the wetting behavior of the material when applied as a biomedical implant. The contact angle for Ti64 alloy is high (80°) (Fig. 5 (a, b)), which decreases gradually on treatment with NaOH solution (25°). Initially at lower atomic % of silver ions the wetness is found to be increased but with further increase of silver ions at the surface the material becomes hydrophobic (Fig. 5 (b)) i.e. the wetness decreases<sup>66</sup>. The present optimized silver concentration (Ti64-N-0.05Ag) is having a lower contact angle

comparing to the Ti64 alloy and Ti64-N surface. Thus we were able to achieve a highly hydrophilic surface on Ti64 alloy by a simple chemical treatment with NaOH and AgNO<sub>3</sub> solutions.

Further bioactivity study in SBF showed that Ti-64 alloy did not form bone like apatite. However, NaOH treated Ti64 alloy formed apatite and the apatite-forming ability did not decrease even Na<sup>+</sup> ions are replaced by Ag<sup>+</sup> ions (Fig. 8 (a)). It is well known that Na<sup>+</sup> ions release into the SBF to form negatively charged Ti-OH group that attracts the positively charged Ca<sup>2+</sup> ions and then negatively charged PO<sub>4</sub><sup>3-</sup> ions to form the bone-like apatite layer. Similar mechanism can be expected in Ti64 alloy containing Ag<sup>+</sup> ions. Interestingly, the bioactivity was not decreased even after heat treatment. It has been already reported that NaOH treatment forms porous SHT layer which has very low scratch resistance.<sup>52</sup> However, on heat treatment around 600 °C, a TiO<sub>2</sub> layer is formed below the titanate network structure that improves the bonding of the network through this TiO<sub>2</sub> layer and increase the scratch resistance<sup>67</sup>. This indicates heat treatment is highly essential to stabilize the porous network structure and surface of the implant subjected to such chemical and heat treatment will not be destroyed during the implantation.<sup>52, 68</sup>

From the present study we observed that the release of Na<sup>+</sup> / Ag<sup>+</sup> ions accelerates the apatite deposition on chemically treated Ti64 alloy. From the AAS result we can see that the amount of Ag<sup>+</sup> ion released from 0.05 mM AgNO<sub>3</sub> treated Ti64 surface, within a period of 24 h, is in the range of 4-5 ppm (Fig. 6 (d)). The antibacterial activity of the same surface against *Staphylococcus aureus* is confirmed by the formation of inhibition zone (Fig. 6 (c)). Although, Ag<sup>+</sup> ion release shows antibacterial effect, excess Ag<sup>+</sup> ion may cause toxicity to the cells<sup>27, 69-74</sup>. Therefore, it is essential to optimize the Ag<sup>+</sup> ion on the Ti64 alloy surface. Present studies show that up to 0.05 mM AgNO<sub>3</sub> samples has

more than 80 % cell viability. Above 0.05 mM, samples showed a decrease in cell viability in the culture medium (Fig. 7 (a)), indicating that 0.05 mM AgNO<sub>3</sub> is an optimum silver concentration which shows both antibacterial property as well as cytocompatibility. Thus bioactive Ti64 alloy coupled with antibacterial behavior and cell viability could be provided by such a simple chemical treatment approach and this method is expected to be useful in development of orthopedic and dental devices.

## 5. Conclusions

Silver ions could be successfully incorporated into the sodium titanate layer formed on Ti64 alloy by NaOH and subsequent AgNO<sub>3</sub> treatment. The resultant silver titanate layer release Ag<sup>+</sup> ions into the surrounding and showed the antibacterial activity against *Staphylococcus aureus*. Further, *in vitro* bioactivity of thus treated Ti64 alloy in simulated body fluid showed bone-like apatite formation within 7 days soaking and this apatite-forming ability is not affected by either silver content or by heat treatment. Cell viability study in MG 63 cell line showed more than 80 % cell viability indicating the non-toxic behavior of the samples. NaOH treatment forms hydrophilic surface and the hydrophilicity is not affected for the present optimum silver concentration. This surface modification study to provide bioactive Ti64 alloy coupled with antibacterial property is expected to have considerable potential in orthopedic and dental implants.

## Acknowledgements

Present authors would like to acknowledge Department of Science and Technology (DST), New Delhi, India (SERB; Fast track research grant no SB/FTP/ETA-257/2012, GAP 11/13) and start up research grant OLP 0083 for the research grant. Support from Central Instrument Facility (CIF) staff Mr. R. Ravishankar, Ms. Nalini (SEM in charge) and Mr. J. Kennedy (XPS in charge) is greatly appreciated. AR

acknowledges UGC for providing the fellowship to carry out the work. DKP acknowledges Prof. T. Matsushita, Chubu University, Japan for providing the samples.

## References

- 1 D. Williams, *Biomaterials*, 2009, **30**, 5897-5909.
- 2 D. M. Brunette, P. Tengvall, M. Textor and P. Thomsen, *Titanium in medicine: material science, surface science, engineering, biological responses and medical applications*, Springer, Germany, 2001.
- 3 T. Kokubo, *Bioceramics and Their Clinical Applications*, ed. Wood head publishing, Sawston, UK, 2008, pp. 784.
- 4 *Metals for Biomedical Devices*, ed. M. Niinomi, Wood head Publishing, UK, 2010.
- 5 K. Bordji, J. Y. Jouzeau, D. Mainard, E. Payan, P. Netter, K. T. Rie, T. Stucky and M. Hage-Ali. *Biomaterials*, 1996, **17**, 929-940.
- 6 D. K. Pattanayak, A. Fukuda, T. Matsushita, M. Takemoto, S. Fujibayashi, K. Sasaki, N. Nishida, T. Nakamura and T. Kokubo, *Acta Biomaterialia*, 2011, **7**, 1398-1406.
- 7 X. Liu, P. K. Chu and C. Ding, *J. Mat. Sci. and Eng. R.*, 2004, **47**, 49-121.
- 8 P. J. Henry, *Int. J. Oral Maxillofac Implants*, 1987, **2**, 23-27.
- 9 J. Lausmaa, B. Kasemo, and H. Mattsson, *Appl. Surf. Sci.*, 1990, **4**, 133-146.
- 10 D. S. Sutherland, P. D. Forshaw, G. C. Allen, I. T. Brown and K. R. Williams, *Biomaterials*, 1993, **14**, 893-899.
- 11 J. P. Lucchini, J. L. Aurelle, M. Therin, K. Donath and W. Becker, *Clin. Oral Implants Res.*, 1996, **7**, 397-404.
- 12 B. Hignett, T. C. Andrew, W. Downing, E. J. Duwell, J. Belanger, E. H. Tulinski, *Surface cleaning, finishing and coating*, ed. W. G. Wood, *Metals Handbook*, American Society for Metals, Metals Park, OH, 1987, vol. **5**, pp.107-127.

- 13 D. Buser, T. Nydegger, T. Oxland, D. L. Cochran, R. K. Schenk, H. P. Hirt, D. Snetivy and L. P. Nolte, *J. Biomed. Mater. Res.*, 1999, **45**, 75-83.
- 14 M. Baleani, M. Viceconti, and A. Toni, *Artif. Organs*, 2000, **24**, 296-299.
- 15 I. Degasne, M. F. Basle, V. Demais, G. Hure, M. Lesourd, B. Grolleau, L. Mercier and D. Chappard, *Calcif. Tissue Int.*, 1999, **64**, 499-507.
- 16 H. B. Wen, J. G. Wolke, J. R. Wijn, Q. Liu, F. Z. Cui and K. De Groot, *Biomaterials*, 1997, **18**, 1471-1478.
- 17 H. B. Wen, Q. Liu, J. R. Wijn and K. De Groot, *J. Mater. Sci. Mater. Med.*, 1998, **9**, 121-128.
- 18 D. K. Pattanayak, S. Yamaguchi, T. Matsushita, T. Nakamura and T. Kokubo, *J. R. Soc. Interface*, 2012, **9**, 2145-2155.
- 19 T. Kawai, M. Takemoto, S. Fujibayashi, H. Akiyama, M. Tanaka, S. Yamaguchi, D. K. Pattanayak, K. Doi, T. Matsushita, T. Nakamura, T. Kokubo and S. Matsuda, *Plos one*, 2014, **9**, e88366.
- 20 P. Tengvall and I. Lundstro, *Clin. Mater.*, 1992, **9**, 115-134.
- 21 D. K. Pattanayak, T. Matsushita, K. Doi, H. Takadama, T. Nakamura and T. Kokubo. *J. Mat. Sci. and Eng. C.*, 2009, **29**, 1974-1978.
- 22 H. M. Kim, F. Miyaji, T. Kokubo and T. Nakamura, *J. Biomed. Mater. Res.*, 1996, **32**, 409-417.
- 23 L. Jonasova, F. A. Muller, A. Helebrant, J. Strnad and P. Greil, *Biomaterials*, 2002, **23**, 3095-3101.
- 24 S. Nishiguchi, T. Nakamura, M. Kobayashi, H. M. Kim, F. Miyaji and T. Kokubo, *Biomaterials*, 1999, **20**, 491-500.
- 25 C. Ohtsuki, H. Iida, S. Hayakawa and A. Osaka, *J. Biomed. Mater. Res.*, 1997, **35**, 39-47.

- 26 S. Kaneko, K. Tsuru, S. Hayakawa, S. Takemoto, C. Ohtsuki, T. Ozaki, H. Innoue and A. Osaka, *Biomaterials*, 2001, **22**, 875-881.
- 27 A. Rajendran and D. K. Pattanayak, *RSC Adv.*, 2014, **4**, 61444-61455.
- 28 X. Wang, S. Hayakawa, K. Tsuru and A. Osaka, *J. Biomed. Mater. Res.*, 2001, **54**, 172-178.
- 29 C. A. B. Nava-Ortiz, G. Burillo, A. Concheiro, E. Bucio, N. Matthijs, H. Nelis, T. Coenye and C. Alvarez Lorenzo, *Acta Biomaterialia*, 2010, **6**, 1398-1404.
- 30 D. S. Jones, C. P. Lorimer, C. P. McCoy and S. P. Gorman, *J. Biomed. Mater. Res Part B: Applied Biomaterials*, 2008, **85**, 417-426.
- 31 L. Zhao, P. K. Chu, Y. Zhang and Z. Wu, *J. Biomed. Mater. Res.: Applied Biomaterials*, 2009, **91B**, 470-480.
- 32 P. Edupungati Om, V. Antoci, S. B. King, B. Jose, C. S. Adams, J. Parvizi, I. M. Shapiro, A. R. Zeiger, N. J. Hickok and E. Wickstrom, *Bioorganic & Medicinal Chemistry Letters*, 2007, **17**, 2692-2696.
- 33 B. Jose, V. Antoci, A. R. Zeiger, E. Wickstrom and N. J. Hickok, *Chemistry & Biology*, 2005, **12**, 1041-1048.
- 34 S. Radin, J. T. Campbell, P. Ducheyne and J. M. Cuckler, *Biomaterials*, 1997, **18**, 777-782.
- 35 M. K. Narbat, J. Kindrachuk, DuanKe, H. Jenssen, R. E. W. Hancock and R. Wanga, *Biomaterials*, 2010, **31**, 9519-9526.
- 36 Z. Wang, Y. Sun, D. Z. Wang, H. Liu and R. I. Boughton, *Int. J. of Nanomed.*, 2013, **8**, 2903-2916.
- 37 Y. Inoue, M. Uota, T. Torikai, T. Watari, I. Noda, T. Hotokebuchi and M. Yada, *J. Biomed. Mater. Res.*, 2010, **92A**, 1171-1180.

- 38 K. Tamai, K. Kawate, I. Kawahara, Y. Takakura and K. Sakaki, *J. Orthop. Sci.*, 2005, **14**, 204-209.
- 39 A. Rajendran, G. Vinoth, V. Shanthi, R. C. Barik, and D. K. Pattanayak, *Mater. Technol.*, 2014, **29**, B26-B34.
- 40 J. S. Patel, S. V. Patel, N. P. Talpada, H and A. Patel, *Mater. and Engg.*, 1999, **271**, 24-27.
- 41 P. V. Asharani, M. G. L. Kah, M. P Hande and S. Valiyaveetil, *ACS Nano*, 2009, **3**, 279-290.
- 42 Y. Mitsunori, I. Yuko, N. Iwao, M. Tomohiro, T. Toshio, W. Takanori, and H. Takao, *J. of Nanomat.*, 2013, 1-9.
- 43 N. Ren, R. Li, L. Chen, G. Wang, D. Liu, Y. Wang, L. Zheng, W. Tang, X. Yu, H. Jiang, H. Liu and N. Wu, *J. Mater. Chem.*, 2012, **22**, 19151- 19160.
- 44 W. Zheng, S. Yan, W. Dongzhou, L. Hong and B. I. Robert, *Int. J. of Nanomed*, 2013, **8**, 2903-2916.
- 45 S. Ferraris, A. Venturello, M. Miola, A. Cochis, L. Rimondini, and S. Spriano, *Appl. Surf. Sci.*, 2014, **311**, 279-291.
- 46 D. Gerlier and N. Thomasset, *J. Immunological Methods*, 1986, **94**, 57-63.
- 47 W. Chrzanowski, N. E. A. Abou, D. A. Armitage, X. Zhao, J. C. Knowles and V. J. Salih, *J. Biomed. Mater. Res. Part A.*, 2010, **93**, 1596-1608.
- 48 T. Kokubo and H. Takadama, *Biomaterials*, 2006, **27**, 2907-2915.
- 49 S. Yamaguchi, T. Matsushita and T. Kokubo, *RSC Adv*, 2013, **3**, 11274-11282.
- 50 J. W. Park, Y. J. Kim, J. H. Jang and H. Song, *Clin. Oral Impl. Res.*, 2010, **21**, 1278-1287.
- 51 T. Kizuki, H. Takadama, T. Matsushita, T. Nakamura and T. Kokubo, *J. Mater. Sci. Mater. Med.*, 2013, **24**, 635-644.

- 52 D. K. Pattanayak, T. Kawai, T. Matsushita, H. Takadama, T. Nakamura and T. Kokubo, *J. Mater. Sci. Mater. Med.*, 2009, **20**, 2401-2411.
- 53 G. V. Rodriguez, A. S. Obregon, S. L. M. Lozano, S. W. Lee, *J. Mol. Catal. A Chem.*, 2012, **353**, 163-170.
- 54 R. Ma, K. Fukuda, T. Sakaki, M. Osada, and Y. Bando, *J. Phys. Chem. B.*, 2005, **109**, 6210-6214.
- 55 T. Kasuga, M. Hiramatsu, A. Hoson, T. Sekino and K. Niihara, *Adv. Mater.*, 1999, **11**, 1307-1311.
- 56 Q. Wang, Y. Zhang, K. Yang and L. Tan, *Surf. Rev. Lett.*, 2009, **16**, 775-779.
- 57 Y. J. Lim, Y. Oshida, C. J. Andres and M. T. Barco, *Int. J. Oral. Maxillofac. Implants*, 2001, **16**, 333-342.
- 58 A. B. G. Lansdown, *J. Wound Care*, 2002, **11**, 125-130.
- 59 Q. L. Feng, J. Wu, G. Q. Chen, F. Z. Cui, T. N. Kim and J. O. Kim, *J. Biomed. Mater. Res.*, 2000, **52**, 662-668.
- 60 M. H. Hermans, *Adv. Skin Wound Care*, 2007, **20**, 166-173.
- 61 X. Wu, L. Jidong, L. Wang, D. Huang, Y. Zuo and L. Yubao, *Biomed. Mater.*, 2010, **5**, 44-105.
- 62 M. Yoshinari, Y. Oda, T. Kato and K. Okuda, *Biomaterials*, 2001, **22**, 2043-2048.
- 63 S. L. R. da. Silva, L. O. Kerber, L. Amaral and C. A. Dos Santos, *Surface and Coatings Technol.*, 1999, **116-119**, 342-346.
- 64 G. B. De Souza, C. M. Leipienski, C. E. Foerster, N. K. Kuromoto, P. Soares and H. De A Ponte, *J. Mech. Behavior of Biomed. Mater.*, 2011, **4**, 756-765.
- 65 S. R. Paital and N. B. Dahotre, *J. Mater. Sci. Eng. R*, 2009, **66**, 1-70.
- 66 S. Kasraei and M. Azarsina, *Braz. Oral. Res.*, 2012, **26**, 505-510.



- 67 S. Nishiguchi, T. Nakamura, M. Kobayashi, H. M. Kim, F. Miyaji and T. Kokubo, *Biomaterials*, 1999, **20**, 491-500.
- 68 D. K. Pattanayak, S. Yamaguchi, T. Matsushita and T. Kokubo, *J. Mat. Sci. Mater. Med.*, 2011, **22**, 1803-1812.
- 69 C. N. Kraft, M. Hansis, S. Arens, M. D. Menger and B. Vollmar, *J. Biomed Mater. Res.*, 2009, **49**, 192-199.
- 70 G. Gosheger, J. Hardes, H. Ahrens, A. Streitburger, H. Buerger, M. Erren, A. Gonsel, F. H. Kemper, W. Winkelmann and C. V. Eiff, *Biomaterials*, 2004, **25**, 5547-5556.
- 71 H. Cao, X. Liu, F. Meng and P. K. Chu, *Biomaterials*, 2011, **32**, 693-705.
- 72 Y. Chen, X. Zheng, Y. Xie, C. Ding, H. Ruan and C. Fan, *J. Mater. Sci. Mater. Med.*, 2008, **19**, 3603-3609.
- 73 J. Liao, M. Anchun, Z. Zhu and Y. Quan, *Int. J. Nanomedicine*, 2010, **5**, 337-342.
- 74 T. Kizuki, T. Matsushita and T. Kokubo, *J Mater. Sci: Mater. Med.*, 2014, **25**, 1737-1746.

### Figure Captions

Fig. 1: SEM images of Ti64 alloy after treatment with NaOH solution and then subsequently soaked in AgNO<sub>3</sub> solutions at different magnifications.

Fig. 2: EDX results of Ti64 alloy after treatment with NaOH solution and then subsequently soaked in different concentrations of AgNO<sub>3</sub> solution.

Fig. 3: (a) and (b) Raman spectra of Ti64 alloys subjected to NaOH solution and subsequently by different concentrations of AgNO<sub>3</sub> treatment before and after heat treatment and (c) Typical XRD pattern of Ti64 alloy subjected to NaOH, NaOH-100Ag and heat treatment.

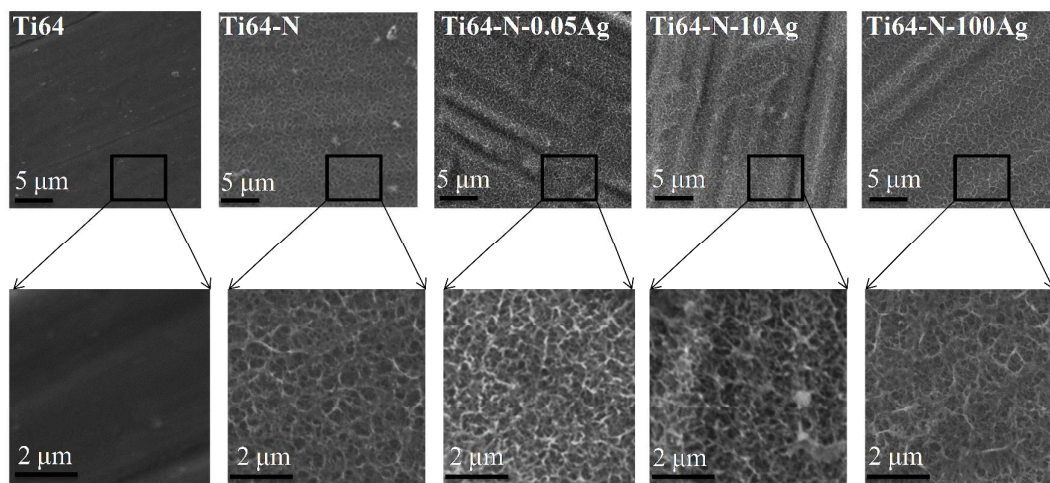
Fig. 4: XPS survey spectrum for Ti64 alloy subjected to NaOH-0.05Ag and heat treatment. The XPS spectra for Ag3d 5/2 and Ag 3d 3/2 is shown as inset.

Fig. 5: (a) Photographs of contact angle measured for Ti64 alloy after treatment with NaOH solution and then subsequently soaked in different concentrations of AgNO<sub>3</sub> solution and (b) its graphical representation.

Fig. 6: (a-c) Disk diffusion test for Ti64 alloy after treatment with NaOH solution and then subsequently soaked in different concentrations of AgNO<sub>3</sub> solution and (d) Silver release from Ti64 alloy treated with NaOH-0.05Ag in SBF.

Fig. 7: (a) MG63 cell viability for Ti64 alloy after treatment with NaOH solution and then subsequently soaked in different concentrations of AgNO<sub>3</sub> solution by MTT assay and (b) SEM image of MG63 cell adhesion on typical silver containing Ti64 alloy surface.

Fig. 8 (a): SEM images of Ti64 alloy with NaOH and different concentration of AgNO<sub>3</sub> treatment before and after heat treatment and soaked in SBF for 7 days and (b) a typical XRD pattern of apatite formed silver containing Ti64 alloy surface.



**Fig. 1:**

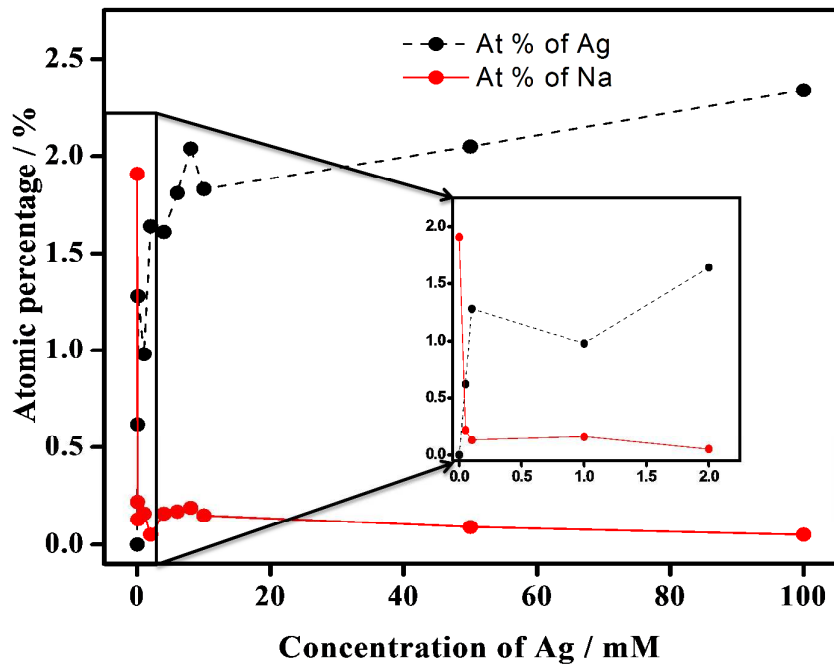


Fig. 2:

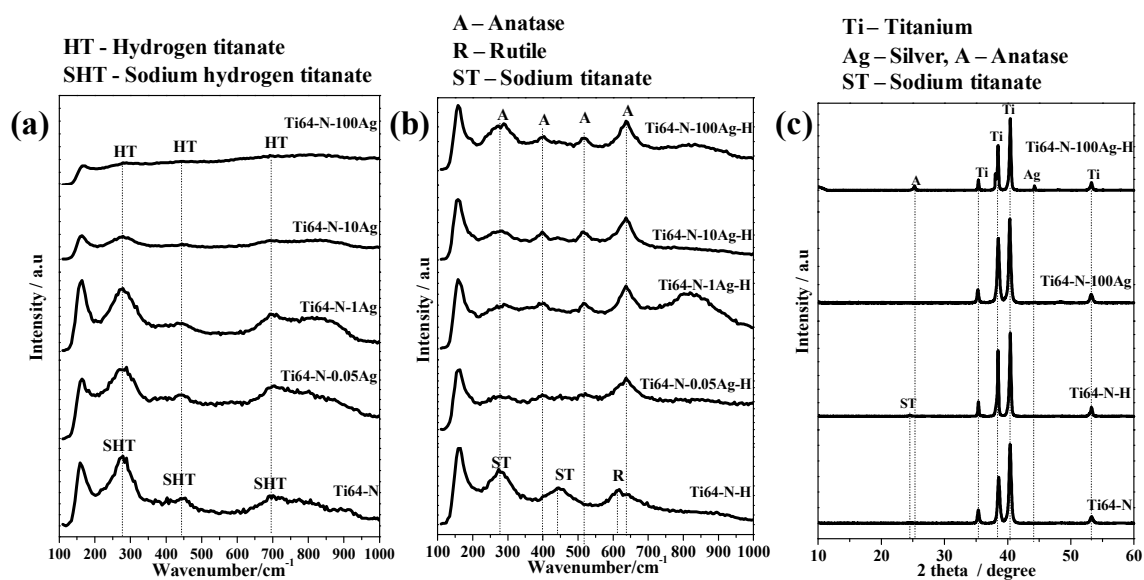


Fig. 3:

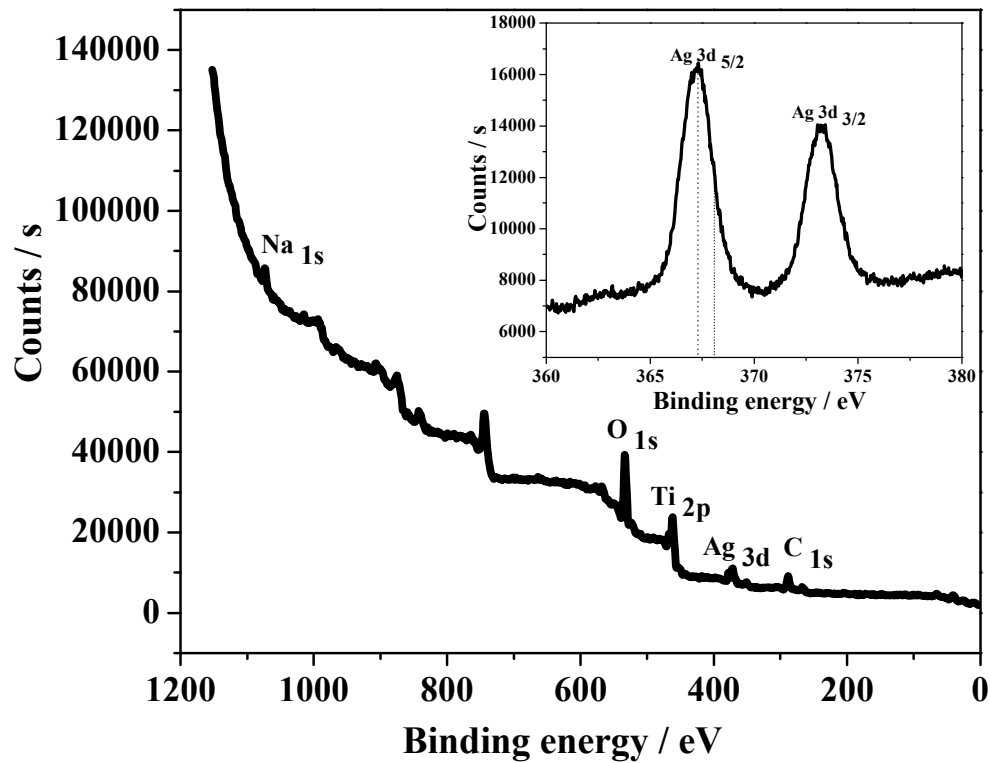


Fig. 4:

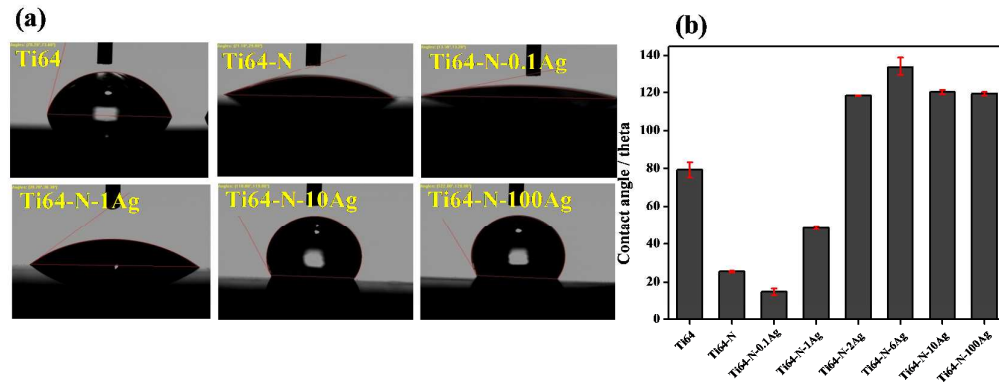


Fig. 5:

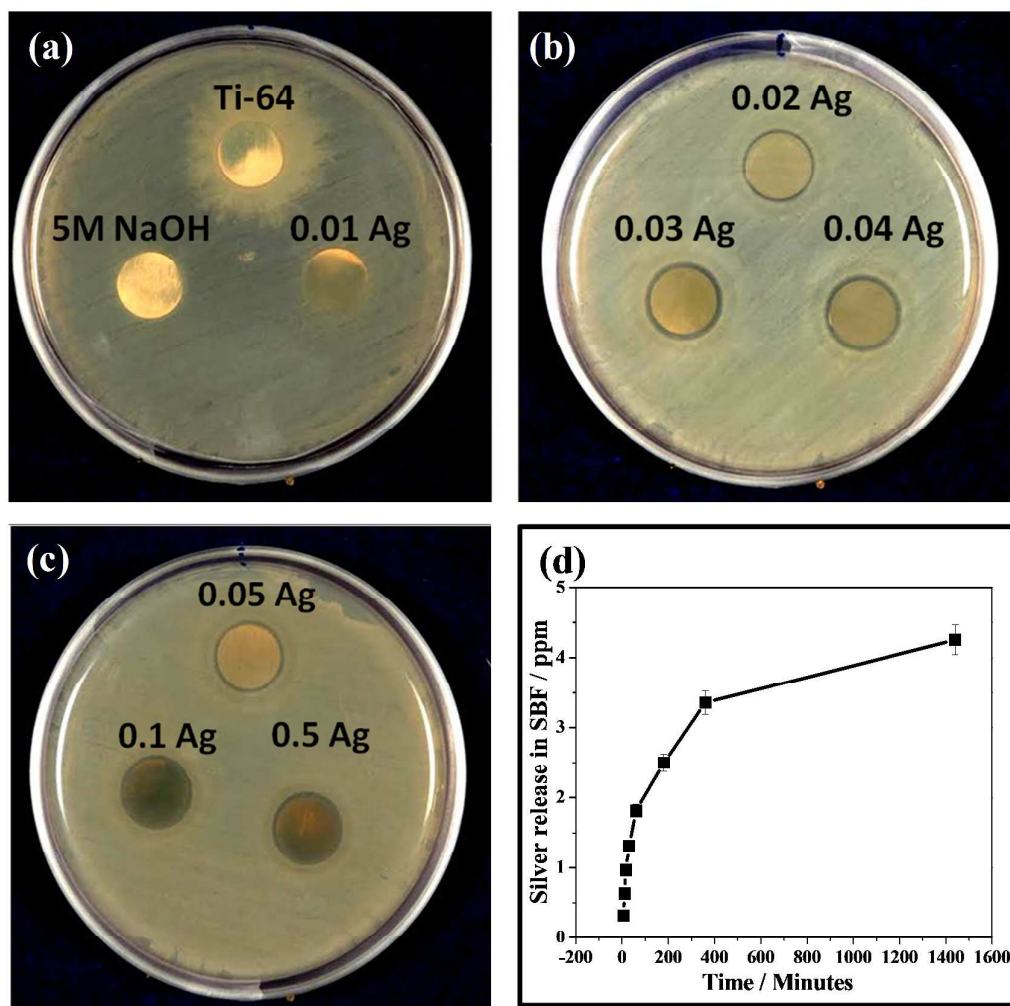


Fig. 6:



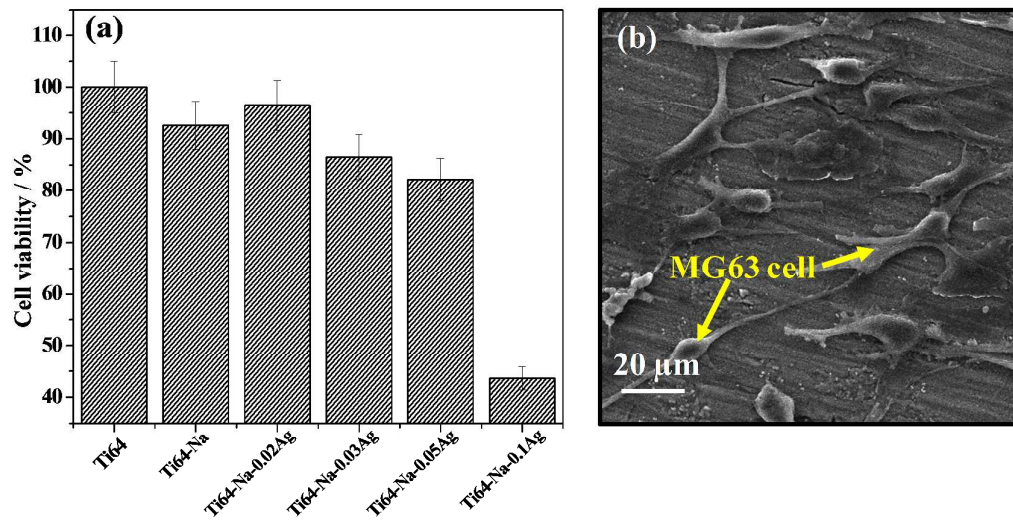


Fig. 7:

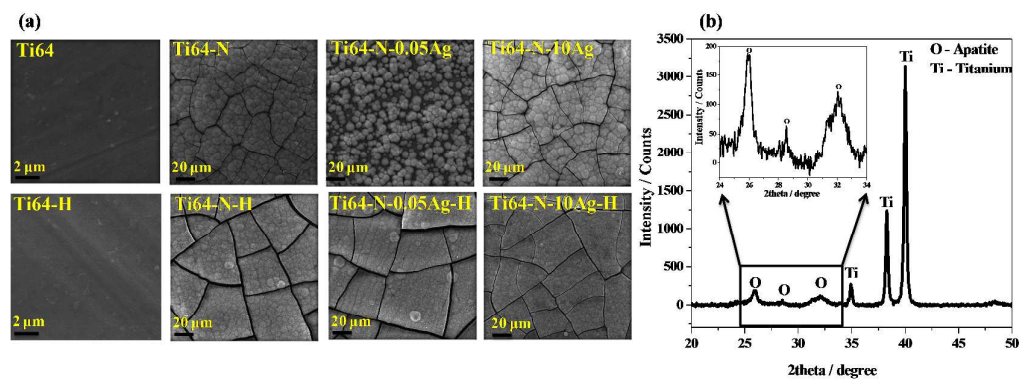


Fig. 8:

**Table 1: Notations for various chemical treatments used in the present study**

| Chemical treatments   | Notations           |
|---|---------------------|
| Untreated Ti -6Al-4V alloy (as-polished)  | Ti64                |
| Ti-6Al-4V alloy treated with 5 M NaOH solutions,<br>60 °C, 24 h   | Ti64-N              |
| Ti-6Al-4V alloy treated with 5 M NaOH solutions,<br>60 °C, 24 h and 0.01-100 mM AgNO <sub>3</sub> solution,<br>40 °C, 24 h                              | Ti64-N-0.01-100Ag   |
| Ti -6Al-4V alloy, heat treated at 600 °C, 1 h   | Ti64-H              |
| Ti-6Al-4V alloy treated with 5 M NaOH solutions,<br>60 °C, 24 h, heat treated at 600 °C, 1 h  | Ti64-N-H            |
| Ti-6Al-4V alloy treated with 5 M NaOH solutions,<br>60 °C, 24 h and 0.01-100 mM AgNO <sub>3</sub> solution,<br>40 °C, 24 h, heat treated at 600 °C, 1 h | Ti64-N-0.01-100Ag-H |

**Table 2: Measured diameter of inhibition zone formed for each sample.**

| <b>Sample notations</b> | <b>Diameter of zone<br/>(including specimen<br/>diameter (1.5cm) )<br/>(cm)</b> | <b>Area of inhibition zone<br/>(<math>A = \pi d^2 / 4</math>)<br/>(cm<sup>2</sup>)</b> |
|-------------------------|---|--|
| Ti64-N-0.02 Ag          | 1.60  | 2.0096   |
| Ti64-N-0.03 Ag          | 1.70  | 2.2687   |
| Ti64-N-0.04 Ag          | 1.80  | 2.5434   |
| Ti64-N-0.05 Ag          | 1.85  | 2.6867   |
| Ti64-N-0.1 Ag           | 1.90  | 2.8338   |
| Ti64-N-0.5 Ag           | 1.92  | 2.8938   |

Schematic representation of Ti64 alloy with antibacterial activity, bioactivity and cell compatibility

